Published in final edited form as:
Cancer. 2014 June 15; 120(12): 1800–1809. doi:10.1002/cncr.28646.

Elevated HA and HMMR are associated with biochemical failure in patients with intermediate grade prostate tumors

Anthony E Rizzardi, BS[1,2], **Rachel Isaksson Vogel, MS**[3], **Joseph S Koopmeiners, PhD**[3,4], **Colleen L Forster, BS**[5], **Lauren O Marston, BS**[2], **Nikolaus K Rosener, BS**[2], **Natalia Akentieva, PhD**[6], **Matthew A Price, BS**[2], **Gregory J Metzger, PhD**[7], **Christopher A Warlick, MD**[8], **Jonathan C Henriksen, BS**[1,2,5], **Eva A Turley, PhD**[6,9,*], **James B McCarthy, PhD**[2,*], and **Stephen C Schmechel, MD, PhD**[1,2,5,*]

[1]Department of Pathology, University of Washington, Seattle, WA

[2]Department of Laboratory Medicine and Pathology and Masonic Cancer Center, University of Minnesota, Minneapolis, MN

[3]Biostatistics and Bioinformatics Core, Masonic Cancer Center, University of Minnesota, Minneapolis, MN

[4]Division of Biostatistics, School of Public Health, University of Minnesota, Minneapolis, MN

[5]BioNet, Academic Health Center, University of Minnesota, Minneapolis, MN

[6]Department of Biochemistry, London Health Sciences Center, University of Western Ontario, London, Ontario, Canada

[7]Department of Radiology, University of Minnesota, Minneapolis, MN

[8]Department of Urology, University of Minnesota, Minneapolis, MN

[9]Department of Oncology, London Health Sciences Center, University of Western Ontario, London, Ontario, Canada

Abstract

Background—The clinical course of prostate cancer (PCa) measured by biochemical failure (BF) after prostatectomy remains unpredictable in many patients, particularly in intermediate Gleason score (GS) 7 tumors, suggesting that identification of molecular mechanisms associated with aggressive PCa biology may be exploited for improved prognostication or therapy. Hyaluronan (HA) is a high molecular weight polyanionic carbohydrate produced by synthases (HAS1-3) and fragmented by oxidative/nitrosative stress and hyaluronidases (HYAL1-4, SPAM1) common in PCa microenvironments. HA and HA fragments interact with receptors CD44 and HMMR resulting in increased tumor aggressiveness in experimental PCa models. We evaluated the association of HA-related molecules with BF after prostatectomy in GS7 tumors.

Corresponding Author: Stephen C Schmechel, MD, PhD, Department of Pathology, University of Washington, Mailcode 359791, 908 Jefferson St, Seattle, WA 98104; Fax: 206-744-8240; sschmech@uw.edu.
*Drs. Turley, McCarthy, and Schmechel are co-last authors

Disclosure/Conflict of Interest: None

Methods—Tissue microarrays were constructed from a 96-patient cohort. HA histochemistry and HAS2, HYAL1, CD44, CD44v6, and HMMR immunohistochemistry were quantified using digital pathology techniques.

Results—HA in tumor-associated stroma and HMMR in malignant epithelium were significantly and marginally significantly associated with time to BF in univariate analysis, respectively. After adjusting for clinicopathologic features, both HA in tumor-associated stroma and HMMR in malignant epithelium were significantly associated with time to BF. Although not significantly associated with BF, HAS2 and HYAL1 positively correlated with HMMR in malignant epithelium. Cell culture assays demonstrated that HMMR bound native and fragmented HA, promoted HA uptake, and was required for a pro-migratory response to fragmented HA.

Conclusions—HA and HMMR are factors associated with time to BF in GS7 tumors, suggesting that increased HA synthesis and fragmentation within the tumor microenvironment stimulates aggressive PCa behavior through HA-HMMR signaling.

Keywords

prostate cancer; biomarkers; digital pathology; hyaluronan; HA; HMMR

Introduction

In 2013, an estimated 239,000 men will be diagnosed with prostate cancer (PCa) and 28,000 men will suffer PCa-specific mortality in the United States.[1] Aggressive PCa is frequently characterized as disease leading to biochemical failure (BF) following prostatectomy, per a standard definition of rising serum PSA after post-operative low nadir proposed by the American Urological Association.[2] Clinical failure defined as systemic progression and/or local tumor recurrence is essentially always preceded by BF, and due to its high sensitivity for clinical failure and routine availability in clinical laboratories worldwide BF can serve as a “gold standard” for PCa outcome.[3]

Recently published clinical trials highlight concerns about overtreatment of men with PCa identified by PSA screening and biopsy since many of these patients have indolent tumors.[4] For example, mathematical modeling studies estimate that without treatment 50–62% of tumors detected through PSA screening and biopsy would not otherwise be clinically recognized, whereas the remaining 38–50% would become symptomatic within 7–14 years after PSA-detected diagnosis.[5] This heterogeneity is especially evident among Gleason score (GS) 7 tumors which contain both Gleason patterns 3 (GP3) and 4 (GP4): GS7 tumors with primary GP3 have an increased biochemical recurrence-free and cancer-specific survival compared to GP4.[6] Recent studies demonstrate extensive chromosomal alterations and molecular heterogeneity between GP3 and GP4 adenocarcinoma further supporting the feasibility of identifying additional molecular targets in PCa.[7]

HA is an extracellular matrix glycosaminoglycan composed of repeating glucuronic acid and N-acetylglucosamine disaccharides. HA signaling is implicated in tumor growth, migration, angiogenesis, and metastasis in PCa.[8] A complex “hyaluronome” that mediates the functions and metabolism of HA consists of HA synthases (HAS1-3), multiple extracellular and

cellular HA binding proteins/receptors, and hyaluronidases (HYAL1-4, SPAM1) which depolymerize HA into fragments of varying sizes.[8] Several lines of evidence suggest that the relative amounts of fragmented HA in tumor-associated stroma critically determine the biological effects of HA on tumor progression. For example, studies using an orthotopic PCa mouse model show that tumor cell expression of HAS2 or HAS3 increases HA accumulation, tumor growth, and angiogenesis.[9] Further, co-expression of HAS2 or HAS3 with HYAL1 (increasing HA fragmentation) is synergistic and results in higher metastatic lymph node tumor burden compared to HAS-only expressing tumor cells.[10] In human tumor specimens, HA (measured using biotinylated HA binding protein; bHABP) and HYAL1 are associated with BF and increased grade.[11,12] Fragmented HA is produced both by local enzymatic action of hyaluronidases and reactive oxygen/nitrogen species,[13] and is common in high grade clinical PCa specimens.[12] Collectively, these data predict that HA is most pathogenic when partially catabolized by local factors within the tumor microenvironment.

The interaction of HA occurs via receptors including CD44 and HMMR. CD44 binds efficiently to native HA and contributes to HA-dependent cell adhesion.[8] Altered expression of variant isoforms, including CD44v6, and downregulation of standard CD44 is notable in many PCa specimens.[14] HMMR is an intracellular protein that is frequently hyper-expressed in tumors and unconventionally exported to the cell surface.[15] HMMR binds efficiently to HA fragments[13,16] and associates with CD44 to regulate signaling resulting in increased motility and invasion.[15,17] Previous studies indicate that increased HMMR correlates with metastatic PCa and development of castration-resistant disease.[18,19]

While the above HA-related gene products are individually implicated in aggressive PCa biology, to our knowledge no study has evaluated these proteins concurrently in GS7 tumors. In this study, we used automated digital pathology methods to quantify staining of HAS2, HA, HYAL1, CD44, CD44v6, and HMMR on tissue microarrays (TMAs) representing GS7 prostatectomy tumors and further evaluated the mechanisms by which HMMR contributes to aggressive PCa in culture assays.

Materials and Methods

Cell lines

C3H/10T1/2 mouse embryonic fibroblasts (MEFs) (ATCC, Manassas, VA) were transfected with mouse HMMR as described.[20] HEK293 cells (Thermo Fisher Scientific, Pittsburg, PA) were cultured in RPMI with 10% FBS. LNCaP cells (ATCC) were cultured in RPMI with 10% FBS. PC3MLN4 cells (provided by Dr. Isaiah Fidler, MD Anderson Cancer Center, Houston, TX) were cultured in DMEM with 10% FBS, sodium pyruvate, and non-essential amino acids (Life Technologies, Carlsbad, CA). Cells were maintained at 37°C in a humidified 5% $C0_2$ incubator.

Western blot analysis

Total protein was quantitated by BCA assay (Thermo Fisher), separated by SDS-PAGE, and transferred to nitrocellulose.[17] For HMMR western blot analysis, a custom mouse monoclonal anti-HMMR (clone 6B7D8; ProMab, Albany, Canada) was prepared

(Supplementary Fig. S2). A HRP-conjugated version (1:900; ProMab) was used in mouse experiments while an unconjugated version (1:900; ProMab) was used for human PC3MLN4 cells. Other antibodies included goat polyclonal anti-HAS2 (Santa Cruz Biotechnologies, Inc., Santa Cruz, CA) and rabbit polyclonal anti-HYAL1 (Sigma). Proteins were detected by ECL (Pierce, Rockford, IL).

Clinical cohort and TMA construction

Archival formalin-fixed paraffin-embedded tissues from patients with combined GS7 (scored for primary GP3 or GP4) prostatic acinar/conventional adenocarcinoma that underwent radical prostatectomy at University of Minnesota Medical Center-Fairview between 1999 and 2008 were collected after approval from the University of Minnesota Institutional Review Board. Demographic and clinical characteristics were abstracted from pathology reports and electronic medical records. TMAs consisting of quadruplicate 1 mm cores of representative PCa areas were constructed using a tissue arrayer (MTA-1; Beecher Instruments Inc., Sun Prairie, WI).

HA histochemistry and HAS2, HYAL1, CD44, CD44v6 and HMMR immunohistochemistry

Full protocol details for immunohistochemistry are available in Supporting Information. HA was histochemically stained using bovine bHABP (Calbiochem, La Jolla, CA). Primary antibodies included HAS2 (Santa Cruz), HYAL1 (Sigma), CD44 (Dako, Glostrup, DK), CD44v6 (R&D Systems, Inc., Minneapolis, MN), and HMMR (ProMab). Reproducibility was assessed by performing a second independent run of immunohistochemistry and image analysis for each biomarker (Supplementary Table S2).

Slide digitization, annotation, and immunohistochemical quantification

Digital images of TMA slides were obtained at 40x magnification (0.0625 μm^2/pixel) with a ScanScope CS (Aperio, Vista, CA) and preprocessed using Genie Histology Pattern Recognition software (Aperio) to classify tissues into Image Classes (tumor, stroma, and glass) as described.[21] DAB staining of HAS2, HYAL1, CD44, CV44v6, and HMMR within tumor epithelium and HA within tumor-associated stroma was quantified using the Color Deconvolution algorithm (Aperio) as the product of staining intensity (average optical density [OD] units) multiplied by the percentage of tumor epithelium or tumor-associated stroma with positive staining (AvgOD*%Pos).[21] The amount of staining present is linearly related to OD.[22]

Statistical analysis

Time to BF was calculated from the date of prostatectomy to BF, defined as the date of a PSA value ≥0.2 ng/mL (>6 weeks after surgery) confirmed by a second PSA value 0.2 ng/mL.[2] BF times were censored at the last contact date for subjects not known to experience BF. Patients without follow-up data other than an initial post-operative PSA value were excluded.

Clinicopathologic features and immunohistochemical staining data (averaged across spots representing each patient) were summarized and their association with BF was evaluated using Cox proportional hazards regression. Clinicopathologic features evaluated included

pre-operative PSA (continuous), age at prostatectomy (continuous), primary GP (3/4), and NonLocalized Tumor Indicator (no/yes) which was defined as extraprostatic extension (pathologic stage pT3+), involved lymph nodes (pN1), and/or positive surgical margins (pR1). The hazard ratio (HR) (per 1 standard deviation difference in biomarker measurement) was used to summarize the association between biomarkers or clinicopathologic features and time to BF. In addition, we completed a Cox proportional hazards analysis to evaluate the association between biomarkers and time to BF adjusted for clinicopathologic features. The association between biomarkers and clinicopathologic features was evaluated using Pearson's coefficient for age and PSA, and the t-test for Gleason score, pathologic stage, lymph node involvement, surgical margin involvement, and Non-Localized Tumor Indicator. Pearson's coefficient was used to evaluate correlation between biomarkers. P-values of ≤ 0.05 were considered statistically significant.

HA pull-down assay

HA pull-down assays using 10 kDa HA conjugated to Sepharose beads were performed as described.[16] Proteins were evaluated by Western blot using rabbit monoclonal anti-HMMR (1:1000; Epitomics, Burlingame, CA).

HA labeling

A HA mixture consisting of oligosaccharides and higher molecular weight (MW) polymers (polydispersity of 5–500 kDa; average: 240 kDa) was labeled with Alexa 647.[23] Subconfluent PC3MLN4 cells were incubated with Alexa 647-HA for 30 min. Cells were fixed in 3% paraformaldehyde at 4°C for 30 min, washed in 1x PBS (pH 7.2), and examined by confocal microscopy (Olympus).

Cell migration assays

Confluent PC3MLN4 cells were scratch wounded, washed with PBS, then maintained in DMEM with 1% FBS. PBS-alone or with dissolved HA fragments (5 μg/mL) were added to wounded monolayers for 24 hours. Cells were fixed in 3% paraformaldehyde and stained with 1% toluidine blue. Cell-free areas were quantified using ImageJ (Bethesda, MD). A peptide mimic (P15) was used to block the HA binding functions of HMMR.[16]

Results

Immunohistochemical analysis of HA metabolic biomarkers in PCa

Data mining and pathway analyses suggested that increased HA metabolism and fragmentation is an important consequence of altered message levels of HAS2, CD44, HMMR, and HYAL1 (Supplementary Table S1 and Supplementary Fig. S1). Therefore, we evaluated these targets on our PCa cohort TMAs in addition to CD44v6 and HA. Verification of staining patterns in control tissues is described in Supporting Information (Supplementary Fig. S3). In PCa tissues, HAS2 displayed coarsely granular cytoplasmic staining (with apical accentuation) in malignant epithelium, and was also detected in stromal fibroblasts (Fig. 1A). HA predominantly exhibited cytoplasmic and extracellular staining around stromal fibroblasts (Fig. 1B) as described.[11,12] HMMR and occasionally HYAL1 exhibited nuclear and finely granular cytoplasmic staining in stromal fibroblasts and

malignant epithelium (Fig. 1C and 1F) as described.[13,15,24] CD44 and CD44v6 displayed crisp membranous staining in malignant epithelium (Fig. 1D and 1E). Fig. 2 depicts the image analysis workflow for tissue classification and staining quantification.

Clinicopathologic features of PCa patients and BF

Adequate tissue was available for 96 subjects for analysis of at least one biomarker. Different TMA spots were missing/excluded during quality control for each stain resulting in varying number of cases with data available for each biomarker (Table 2 below). A Kaplan-Meier curve illustrating time to BF for all subjects is shown in Figure 3. Of 96 patients, 15 failed during follow-up. The median time to BF was 6.9 years (range 0.26–9.60 years). The median follow-up among non-failures was 2.3 years (range 0.14–8.56 years). Non-Localized Tumor Indicator and preoperative PSA were significantly and marginally significantly associated with time to BF, respectively (Table 1). Primary GP and age were not statistically significant; however, multivariate analyses were adjusted for these parameters based on established prognostic clinicopathologic features.[25]

Prognostic significance of HA metabolic biomarkers

Malignant epithelial HMMR was statistically significantly associated with time to BF before adjusting for clinicopathologic features (p=0.028), and stromal HA was marginally-statistically significant (p=0.065) (Table 2). HMMR remained statistically significantly associated (p=0.040) with time to BF and stromal HA became statistically significantly associated (p=0.047) after adjustment for clinicopathologic features. Hazard ratios were similar in both models. Figure 4 shows representative IHC staining of HA and HMMR in BF and non-BF groups. These data demonstrate that HA and HMMR are associated with time to BF in patients with GS7 tumors.

Pairwise correlation of HA metabolic biomarkers

We evaluated the association between biomarkers and all clinicopathologic parameters. Significant associations were observed between HAS2 and surgical margin positivity (p = 0.038), HAS2 and age (p = 0.010), CD44v6 and pathologic stage (0.014), HMMR and Gleason score (p = 0.046), and between HMMR and pathologic stage (p = 0.036).

Associations between HA metabolism biomarkers were evaluated by estimating the pairwise correlations. As shown in Table 3, comparisons between the staining intensity of the selected biomarkers indicated moderate and statistically significant correlations between HAS2 and HYAL1 (correlation=0.443, p<0.0001), HAS2 and HMMR (correlation=0.523, p<0.0001), and HYAL1 and HMMR (correlation=0.456, p<0.0001). Although HAS2 and HYAL1 were not statistically significant in regression models with BF, these results suggest that HMMR expression is linked to that of both HAS2 and HYAL1 which are responsible for HA synthesis and catabolism.

HMMR binds to low MW HA and is essential for fragmented HA-dependent cell migration

Because HA and HMMR were strongly associated with BF, and HMMR expression was linked to HAS2 and HYAL1, we further interrogated a model of HMMR-dependent PCa progression whereby fragmented HA in the tumor microenvironment binds to HMMR to

promote cell proliferation and motility. We confirmed protein expression of key HA pathway components in PC3MLN4 cells including HMMR (Supplementary Fig. S2D) as well as HAS2 and HYAL1 (Fig. 5A). Exposure of PC3MLN4 cells to 6.2 and 10 kDa HA fragments to mimic HA fragmentation in the tumor microenvironment substantially induced cell migration although migration was inhibited by smaller 2.1 kDa HA fragments (Fig. 5B). Similar inhibitory effects using small HA oligosaccharides are evident in other tumor cell lines and linked to their capacity to disrupt HA receptor interactions.[26]

We next assessed whether endogenous HMMR expressed by PC3MLN4 cells mediated the motogenic effects from binding 6.2 and 10 kDa HA fragments. As shown in Fig. 5C, HMMR expressed by PC3MLN4 cells bound efficiently to 10 kDa HA fragments at similar levels to HMMR-transfected 10T1/2 MEFs (positive control), previously demonstrated to bind to HA fragments via HMMR.[16] Furthermore, binding and uptake of Alexa647-labeled HA fragments (10 kDa) was blocked by anti-HMMR antibody indicating that receptor binding of HA fragments specifically occurs through HMMR in PC3MLN4 cells (Fig. 5D). Cell migration assays using HMMR mimetic peptide (P15), previously shown to interfere with HMMR:HA fragment interactions,[16] functionally confirmed that HMMR mediated the motogenic effects of binding HA fragments which supports a role for HMMR:HA fragment interactions in promoting aggressive tumor behavior (Fig. 5E).

Discussion

Understanding the causes of PCa aggressiveness may highlight pathways for prognostics or therapeutics. Prostate tumors often follow an unpredictable clinical course, most notably in GS7 tumors.[6] The present study focused on evaluating the importance of HA metabolic pathway components in these patients and investigating a mechanism by which aberrant HA signaling contributes to PCa progression. While HAS2, HA, HYAL1, CD44, CD44v6, and HMMR have been individually implicated in PCa progression,[10,12,14,19] to our knowledge this is the first report to evaluate these proteins within heterogeneous GS7 tumors. Our results indicated that elevated HA in tumor-associated stroma and HMMR in malignant epithelium were associated with BF in this intermediate risk group (including adjustment for primary GP3/GP4). We also demonstrated that PCa cells migrate in response to HA fragments in a HMMR-dependent manner, suggesting a paracrine mechanism by which elevated HMMR and HA enhance PCa progression.

Tumor-associated HA, which correlated with BF in our cohort of GS7 tumors, has multiple pro-tumorigenic properties that enhance PCa progression.[8] Our findings are supported by previous studies showing that HA and HYAL1 are elevated in advanced PCa.[11,12] Native HA is deposited within tumor-associated stroma by HA synthases where enzymatic (e.g., HYAL1) and physical (e.g., free oxygen/nitrogen radical) mechanisms catabolize HA into heterogeneous sizes which are proinflammatory and angiogenic.[13] Thus, the ratio of intact to degraded HA in the microenvironment directly correlates to the metastatic proclivity of PCa cells, with increased fragmentation leading to metastasis.[10] These studies highlight the consequences of increased HA fragmentation which agree with our results and suggests a mechanism whereby HA and HYAL1 prime the tumor microenvironment to promote PCa progression.

Major cellular receptors for HA identified in PCa include CD44 and HMMR which control numerous oncogenic signal transduction pathways in response to ligation by intact and fragmented HA.[15] Although we did not see a link between standard CD44 with BF in our study, decreased CD44 was associated with increased primary GP in this cohort (4 vs. 3; p=0.043; data not shown) agreeing with prior reports.[14] However, the role(s) of CD44 in PCa formation and progression appear to be complex since CD44 may also function to sustain tumor initiating cells.[27] Alternatively, growth factor-induced upregulation of CD44 variant isoforms such as CD44v9 may be critical for interacting with stromal HA to promote tumor progression.[28] Sorting out this complexity will require further analysis using expanded patient cohorts and refined genomic analysis.

In contrast to CD44, HMMR expression is increased in metastatic PCa[18] and linked to the development of castration-resistant PCa.[19] In this study of GS7 tumors, increased HMMR was associated with decreased time to BF and positively correlated with expression of HAS2 and HYAL1. HMMR is multicompartmentalized and unconventionally exported to the cell surface where it regulates signaling in response to HA by associating with CD44 and other integral receptors (e.g., PDGFR, RON).[15] Loss of CD44 forces HMMR to partner with other as yet unknown receptors, which accelerates cell migration and invasion,[29] and may produce similar effects through increased HMMR and HA fragment interaction. Cell surface HMMR responds to extracellular HA to promote cell motility and motogenic signaling through sustained ERK1/2 activation during tumor cell migration.[17] In contrast, intracellular HMMR binds to the cytoskeleton and MEK1/ERK1/2 complexes which affects mitotic spindle integrity and may contribute to genomic instability during tumor progression.[30] Some evidence suggests that intracellular HMMR actively binds intracellular HA providing an unexplored link between intracellular/extracellular HA signaling and cytoskeletal dynamics.[31] Further studies are in progress to define the functional relationship between intracellular/extracellular HMMR during PCa progression and to relate changes to genomic instability. Collectively, our results strongly support the conclusion that elevated HMMR and HA fragmentation represent a threshold in intermediate grade tumors that portends malignant progression.

It is important to note that a conflicting study recently reported that increased HMMR was associated with a significantly lower risk of BF in primary localized PCa.[18] These findings were speculated to be linked to the immunogenic properties of surface HMMR based on previous work demonstrating a beneficial immune response to surface HMMR in leukemic patients.[32] However, an anti-HMMR immune response was not documented in their PCa studies creating uncertainty as to this potential explanation. While it is premature to conclude that every tumor with increased HMMR leads to poor (or good) outcome, factors related to inter-patient heterogeneity are important variables in these types of studies. Clearly, these discrepancies emphasize the need for additional studies to clarify findings and conclusions.

Although we did not find an association between CD44, CD44v6, or HYAL1 with time to BF, our data support the model of aberrant HA-HMMR signaling in aggressive PCa. Ongoing studies are aimed at expanding the patient cohort to further determine if HA metabolic biomarkers could improve prognosis and support for a HMMR-dependent

mechanistic model of PCa progression. Our laboratories are currently evaluating the potential for small molecules capable of interrupting fragmented HA-HMMR interactions to limit malignant progression, thus providing a therapeutic target to inhibit tumor cell proliferation, angiogenesis, inflammation, and metastasis.

Supplementary Material

Refer to Web version on PubMed Central for supplementary material.

Acknowledgments

The authors thank Dr. Timothy Schacker (supported by NIH grants P01-AI074340, R01-AI093319) for providing computer resources used in this study.

Funding: This work was supported by NIH grants R01-CA119092 (JBM, EAT), R01-CA131013 (GJM), University of Minnesota (UMN) Chairman's Fund Endowed Chair in Cancer Biology (JBM), UMN Biostatistics and BioNet core facilities (supported by P30-CA77598, P50-CA101955, KL2-RR033182, UMN Academic Health Center), UMN Department of Laboratory Medicine and Pathology (SCS), and University of Washington Department of Pathology (SCS).

References

1. Siegel R, Naishadham D, Jemal A. Cancer statistics, 2013. CA Cancer J Clin. 2013; 63:11–30. [PubMed: 23335087]
2. Cookson MS, Aus G, Burnett AL, et al. Variation in the definition of biochemical recurrence in patients treated for localized prostate cancer: the American Urological Association Prostate Guidelines for Localized Prostate Cancer Update Panel report and recommendations for a standard in the reporting of surgical outcomes. J Urol. 2007; 177:540–545. [PubMed: 17222629]
3. Pound CR, Partin AW, Eisenberger MA, Chan DW, Pearson JD, Walsh PC. Natural history of progression after PSA elevation following radical prostatectomy. JAMA. 1999; 281:1591–1597. [PubMed: 10235151]
4. Andriole GL, Crawford ED, Grubb RL 3rd, et al. Prostate cancer screening in the randomized Prostate, Lung, Colorectal, and Ovarian Cancer Screening Trial: mortality results after 13 years of follow-up. J Natl Cancer Inst. 2012; 104:125–132. [PubMed: 22228146]
5. Gulati R, Wever EM, Tsodikov A, et al. What if i don't treat my PSA-detected prostate cancer? Answers from three natural history models. Cancer Epidemiol Biomarkers Prev. 2011; 20:740–750. [PubMed: 21546365]
6. Tollefson MK, Leibovich BC, Slezak JM, Zincke H, Blute ML. Long-term prognostic significance of primary Gleason pattern in patients with Gleason score 7 prostate cancer: impact on prostate cancer specific survival. J Urol. 2006; 175:547–551. [PubMed: 16406993]
7. Kovtun IV, Cheville JC, Murphy SJ, et al. Lineage relationship of Gleason patterns in Gleason score 7 prostate cancer. Cancer Res. 2013; 73:3275–3284. [PubMed: 23695551]
8. Simpson MA, Lokeshwar VB. Hyaluronan and hyaluronidase in genitourinary tumors. Front Biosci. 2008; 13:5664–5680. [PubMed: 18508614]
9. Simpson MA, Wilson CM, McCarthy JB. Inhibition of prostate tumor cell hyaluronan synthesis impairs subcutaneous growth and vascularization in immunocompromised mice. Am J Pathol. 2002; 161:849–857. [PubMed: 12213713]
10. Bharadwaj AG, Kovar JL, Loughman E, Elowsky C, Oakley GG, Simpson MA. Spontaneous metastasis of prostate cancer is promoted by excess hyaluronan synthesis and processing. Am J Pathol. 2009; 174:1027–1036. [PubMed: 19218337]
11. Ekici S, Cerwinka WH, Duncan R, et al. Comparison of the prognostic potential of hyaluronic acid, hyaluronidase (HYAL-1), CD44v6 and microvessel density for prostate cancer. Int J Cancer. 2004; 112:121–129. [PubMed: 15305383]

12. Lokeshwar VB, Rubinowicz D, Schroeder GL, et al. Stromal and epithelial expression of tumor markers hyaluronic acid and HYAL1 hyaluronidase in prostate cancer. J Biol Chem. 2001; 276:11922–11932. [PubMed: 11278412]

13. Slevin M, Krupinski J, Gaffney J, et al. Hyaluronan-mediated angiogenesis in vascular disease: uncovering RHAMM and CD44 receptor signaling pathways. Matrix Biol. 2007; 26:58–68. [PubMed: 17055233]

14. Iczkowski KA. Cell adhesion molecule CD44: its functional roles in prostate cancer. Am J Transl Res. 2010; 3:1–7. [PubMed: 21139802]

15. Maxwell CA, McCarthy J, Turley E. Cell-surface and mitotic-spindle RHAMM: moonlighting or dual oncogenic functions? J Cell Sci. 2008; 121:925–932. [PubMed: 18354082]

16. Tolg C, Hamilton SR, Zalinska E, et al. A RHAMM mimetic peptide blocks hyaluronan signaling and reduces inflammation and fibrogenesis in excisional skin wounds. Am J Pathol. 2012; 181:1250–1270. [PubMed: 22889846]

17. Hamilton SR, Fard SF, Paiwand FF, et al. The hyaluronan receptors CD44 and Rhamm (CD168) form complexes with ERK1,2 that sustain high basal motility in breast cancer cells. J Biol Chem. 2007; 282:16667–16680. [PubMed: 17392272]

18. Gust KM, Hofer MD, Perner SR, et al. RHAMM (CD168) is overexpressed at the protein level and may constitute an immunogenic antigen in advanced prostate cancer disease. Neoplasia. 2009; 11:956–963. [PubMed: 19724689]

19. Korkes F, Castro MG, Zequi SD, Nardi L, ALG, Peo AC. RHAMM immunohistochemical expression and androgen deprivation in normal peritumoural, hyperplasic and neoplastic prostate tissue. BJU Int. 2013

20. Zhang S, Chang MC, Zylka D, Turley S, Harrison R, Turley EA. The hyaluronan receptor RHAMM regulates extracellular-regulated kinase. J Biol Chem. 1998; 273:11342–11348. [PubMed: 9556628]

21. Rizzardi AE, Johnson AT, Vogel RI, et al. Quantitative comparison of immunohistochemical staining measured by digital image analysis versus pathologist visual scoring. Diagn Pathol. 2012; 7:42. [PubMed: 22515559]

22. Krajewska M, Smith LH, Rong J, et al. Image analysis algorithms for immunohistochemical assessment of cell death events and fibrosis in tissue sections. J Histochem Cytochem. 2009; 57:649–663. [PubMed: 19289554]

23. Veiseh M, Breadner D, Ma J, et al. Imaging of homeostatic, neoplastic, and injured tissues by HA-based probes. Biomacromolecules. 2012; 13:12–22. [PubMed: 22066590]

24. Lindwall C, Olsson M, Osman AM, Kuhn HG, Curtis MA. Selective expression of hyaluronan and receptor for hyaluronan mediated motility (Rhamm) in the adult mouse subventricular zone and rostral migratory stream and in ischemic cortex. Brain Res. 2013; 1503:62–77. [PubMed: 23391595]

25. Swanson GP, Basler JW. Prognostic factors for failure after prostatectomy. J Cancer. 2010; 2:1–19. [PubMed: 21197260]

26. Urakawa H, Nishida Y, Knudson W, et al. Therapeutic potential of hyaluronan oligosaccharides for bone metastasis of breast cancer. J Orthop Res. 2012; 30:662–672. [PubMed: 21913222]

27. Patrawala L, Calhoun T, Schneider-Broussard R, et al. Highly purified CD44+ prostate cancer cells from xenograft human tumors are enriched in tumorigenic and metastatic progenitor cells. Oncogene. 2006; 25:1696–1708. [PubMed: 16449977]

28. Ghatak S, Hascall VC, Markwald RR, Misra S. Stromal hyaluronan interaction with epithelial CD44 variants promotes prostate cancer invasiveness by augmenting expression and function of hepatocyte growth factor and androgen receptor. J Biol Chem. 2010; 285:19821–19832. [PubMed: 20200161]

29. Nedvetzki S, Gonen E, Assayag N, et al. RHAMM, a receptor for hyaluronan-mediated motility, compensates for CD44 in inflamed CD44-knockout mice: a different interpretation of redundancy. Proc Natl Acad Sci U S A. 2004; 101:18081–18086. [PubMed: 15596723]

30. Tolg C, Hamilton SR, Morningstar L, et al. RHAMM promotes interphase microtubule instability and mitotic spindle integrity through MEK1/ERK1/2 activity. J Biol Chem. 2010; 285:26461–26474. [PubMed: 20558733]

31. Evanko SP, Parks WT, Wight TN. Intracellular hyaluronan in arterial smooth muscle cells: association with microtubules, RHAMM, and the mitotic spindle. J Histochem Cytochem. 2004; 52:1525–1535. [PubMed: 15557208]

32. Greiner J, Schmitt M, Li L, et al. Expression of tumor-associated antigens in acute myeloid leukemia: Implications for specific immunotherapeutic approaches. Blood. 2006; 108:4109–4117. [PubMed: 16931630]

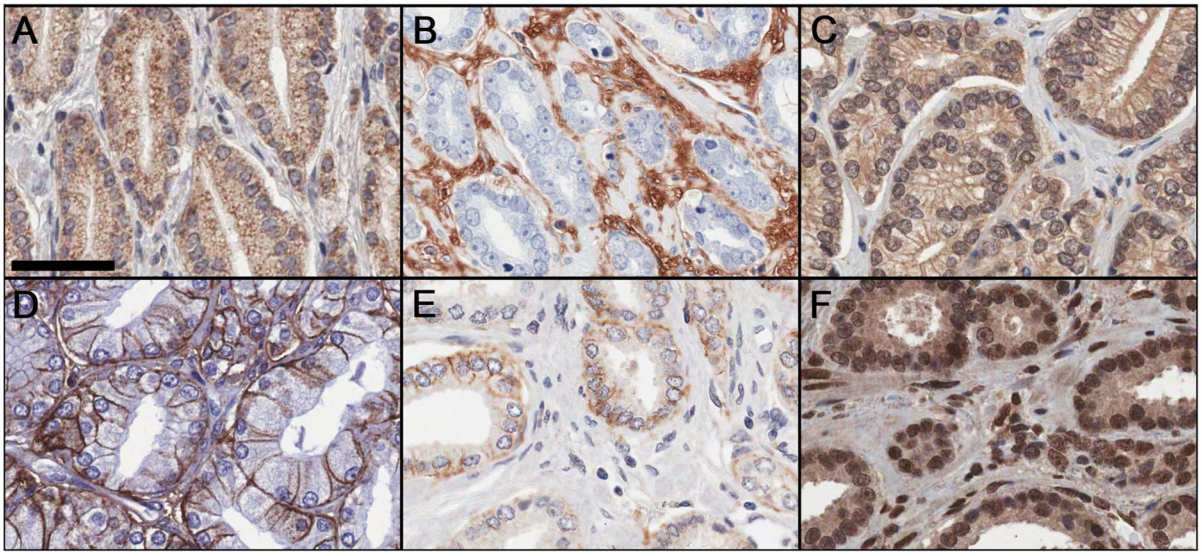

Figure 1.

Representative immunohistochemical staining for HAS2 (A), HA (B), HYAL1 (C), CD44 (D), CD44v6 (E), and HMMR (F) on prostate cancer tissue microarrays. Scale bar represent 50 μm.

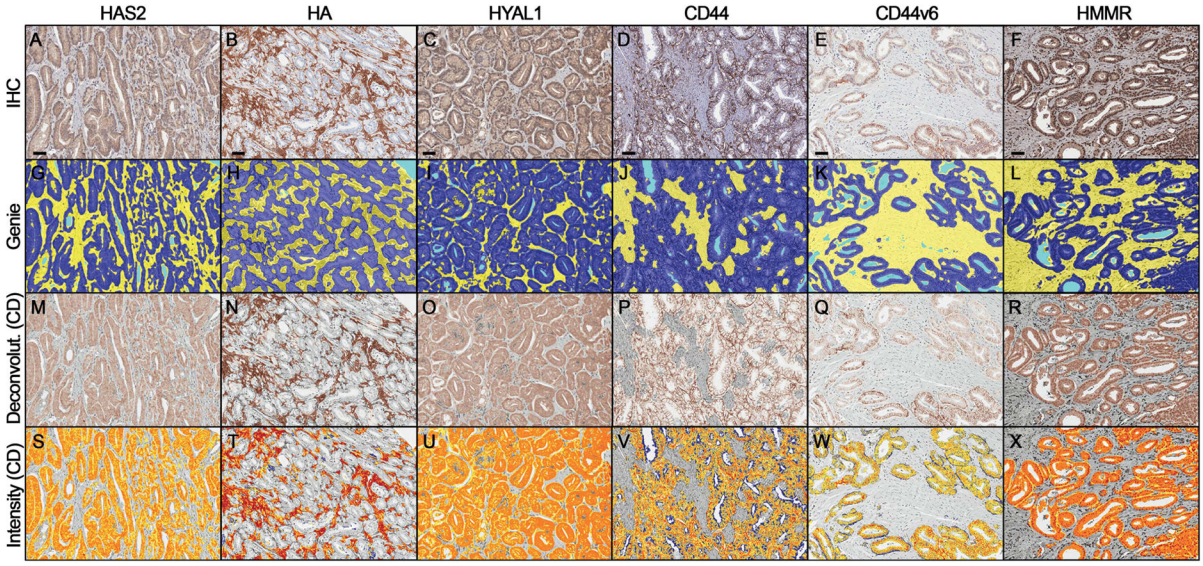

Figure 2.

(A–F) Prostate cancer tissue microarrays were stained by immunohistochemistry. (G–L) Genie Pattern Recognition software (Aperio) subclassified tumor areas into malignant epithelium (dark blue), stroma (yellow), and glass (light blue). (M–R) DAB staining in malignant epithelium (HAS2, HYAL1, CD44, CD44v6 and HMRR) or stroma (HA) was deconvolved from counterstain using Color Deconvolution (Aperio). (S–X) DAB staining was quantified in these areas and pseudocolored for weak (yellow), moderate (orange), and strong (red) staining. Scale bars represent 50 μm.

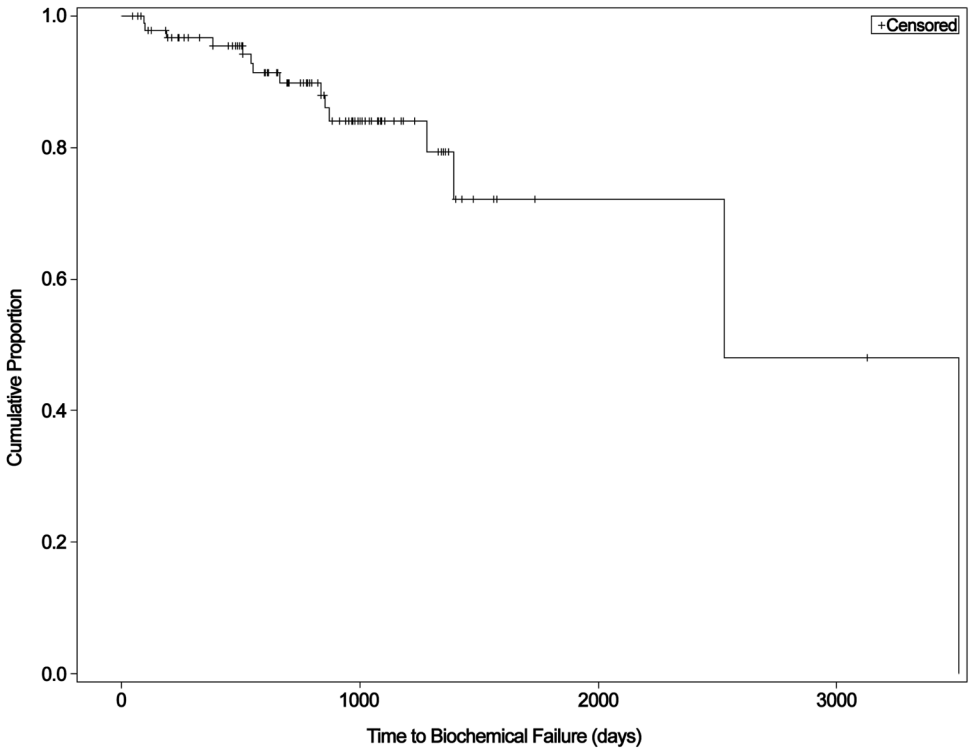

Figure 3.
Kaplan-Meier curve demonstrating the time to biochemical failure for the sample population.

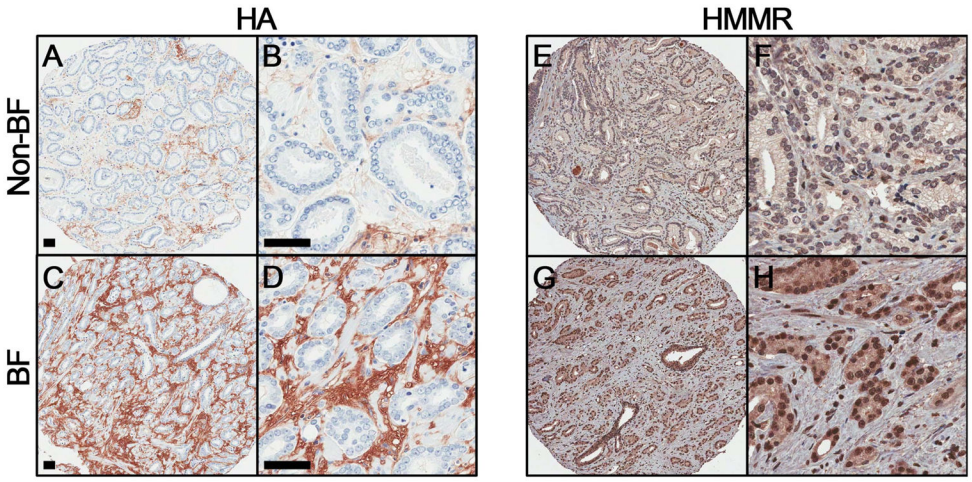

Figure 4.

Representative immunohistochemical staining for HA (A–D) and HMMR (E–H) in biochemical failure (BF) and non-failure (non-BF) groups. Scale bar represent 50 μm.

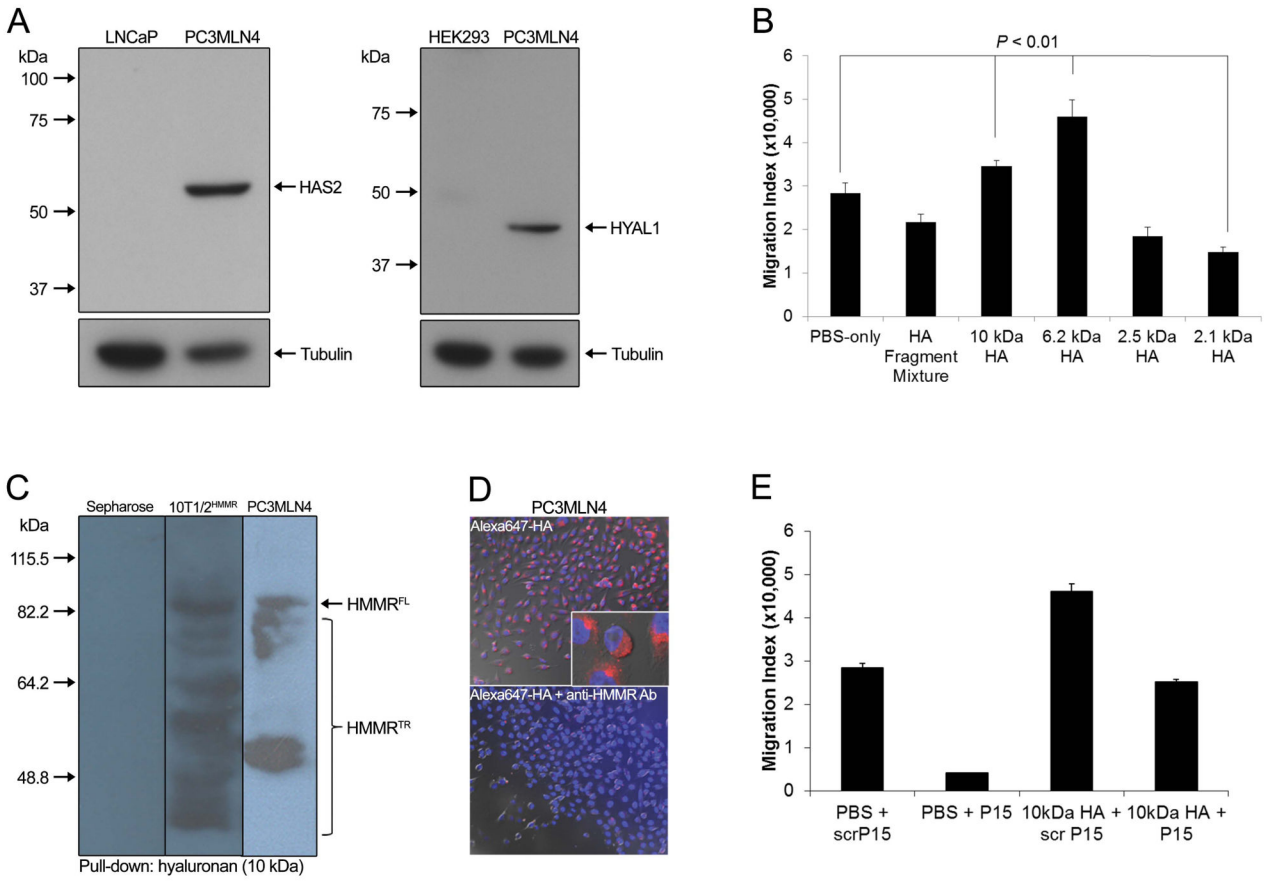

Figure 5.

(A) Western blot analysis confirmed protein expression of HAS2 and HYAL1 in PC3MLN4 cells. (B) Cell migration assays demonstrated increased motility in response to 6.2 and 10 kDa HA (5 μg/mL) and decreased motility in response to 2.1 kDa HA (5 μg/mL) relative to PBS controls. (C) HA pull-down assays were performed with 10 kDa HA coupled to Sepharose beads. Western blot analysis revealed that full-length (FL) and truncated (TR) HMMR expressed by PC3MLN4 cells bound efficiently to 10 kDa HA at similar levels to HMMR-transfected 10T1/2 cells (positive control). (D) PC3MLN4 cells bound and internalized Alexa 647-labeled HA fragments (top) while addition of anti-HMMR antibody blocked binding and uptake of Alexa 647-labeled HA fragments (bottom) detected by fluorescent microscopy. Binding was blocked by excess unlabeled HA and confirmed specificity of labeled HA (data not shown). (E) Cell migration increased in response to 10 kDa HA fragments (5 μg/mL) and was inhibited by HMMR mimetic peptide P15 (20 μg/mL), but not by its scrambled peptide control. Error bars, SEM of triplicate determinations. Statistically significant differences were observed ($p<0.01$) as determined by Student's *t*-test.

Table 1

Association of clinicopathologic features with time to biochemical failure using univariate Cox regression models

Variable	N	%	HR (95%CI)	P-value
Total population	96			
Gleason score				0.937
3+4	63	41.2	0.96 (0.32–2.88)	
4+3	33	21.6	1.00	
Pathologic stage				0.036
Extraprostatic extension (pT3+)	22	22.9	3.26 (1.08–9.80)	
Prostate-limited (pT2)	74	77.1	1.00	
Lymph node involvement				0.116
Yes (pN1)	3	3.1	3.52 (0.74–16.81)	
No (pN0)	93	96.9	1.00	
Surgical margin involvement				0.016
Yes (pR1)	40	41.7	4.86 (1.35–17.54)	
No (pR0)	56	58.3	1.00	
Non-Localized Tumor Indicator*				0.022
Yes	50	52.1	5.75 (1.28–25.74)	
No	46	47.9	1.00	
	N	**Mean (SD)**	**HR (95%CI)**	**P-value**
Age (years)	90	61.1 (6.6)	1.05 (0.97–1.14)	0.257
Pre-operative PSA (ng/mL)	96	7.4 (5.2)	1.06 (1.00–1.13)	0.070

*Non-Localized Tumor Indicator is a summary metric of tumor confined to prostate. ‘Yes’ indicates extraprostatic extension (pathologic stage pT3+), involved lymph nodes (pN1), and/or positive surgical margins (pR1).

Table 2

Biomarkers as predictors of time to biochemical failure using Cox regression models

	Univariate				Multivariate*			
Variable	**N-total**	**N-events**	**HR (95%CI)**	**P-value**	**N-total**	**N-events**	**HR (95%CI)**	**P-value**
HAS2	93	14	1.29 (0.73–2.27)	0.381	87	13	1.66 (0.90–3.03)	0.102
HA	94	15	1.66 (0.97–2.83)	0.065	88	14	1.74 (1.01–2.99)	0.047
HYAL1	93	13	1.54 (0.88–2.68)	0.131	87	12	1.63 (0.86–3.12)	0.136
CD44	92	13	0.87 (0.50–1.54)	0.642	86	12	0.75 (0.42–1.35)	0.339
CD44v6	91	13	1.24 (0.77–2.00)	0.376	85	12	1.34 (0.79–2.26)	0.282
HMMR	89	13	2.00 (1.08–3.71)	0.028	83	12	2.03 (1.04–3.99)	0.040

*Adjusted for age at prostatectomy, preoperative PSA, primary Gleason pattern, and Non-Localized Tumor Indicator.

Cancer. Author manuscript; available in PMC 2015 June 15.

Table 3

Pearson coefficients for correlations between biomarkers

	HAS2	HA	HYAL1	CD44	CD44v6
	0.298				
HA	p=0.004				
	n=93				
	0.443	0.008			
HYAL1	p<0.0001	p=0.937			
	n=91	n=91			
	−0.185	−0.152	−0.139		
CD44	p=0.080	p=0.151	p=0.189		
	n=91	n=91	n=91		
	−0.146	−0.073	−0.173	0.281	
CD44v6	p=0.169	p=0.496	p=0.104	p=0.007	
	n=90	n=90	n=90	n=91	
	0.523	0.236	0.456	−0.001	−0.199
HMMR	p<0.0001	p=0.027	p<0.0001	p=0.992	p=0.063
	n=88	n=88	n=88	n=89	n=88